


 Cite this: *New J. Chem.*, 2025, 49, 4333

# The formation of cyclotriazane (N<sub>3</sub>H<sub>3</sub>) from ammonia in contact with a silver-exchanged LTA zeolite: a reliable synthesis pathway?†

 Rémi Beucher,<sup>a</sup> Pavel Afanasiev,<sup>id</sup><sup>a</sup> Emmanuel Lacôte<sup>id</sup><sup>b</sup> and David Farrusseng<sup>id</sup><sup>\*a</sup>

Sigma-catenated polynitrogen derivatives are scarce. Among polyazanes, the synthesis of derivatives of cyclotriazane (general formula N<sub>3</sub>H<sub>3</sub>) remains a challenge due to their very high reactivity. While several methods toward protected variants of cyclotriazane have been introduced, N<sub>3</sub>H<sub>3</sub> itself has only been observed by Kim and Seff through the stoichiometric oxidation of ammonia on a (Ag<sup>+</sup>)-exchanged LTA zeolite followed by thermodesorption. Based on single-crystal XRD analysis of the crystal, they proposed the presence of cyclotriazane confined in the alpha cavity of the zeolite and in the sodalite cages. Since this 1977 publication by Kim and Seff, we could not find any other publications on this topic, and to the best of our knowledge, triazane has not yet been isolated. In the quest to decipher the mechanism of formation of cyclotriazane, we have studied the reactivity of silver-exchanged LTA zeolites with NH<sub>3</sub> by *operando* DRIFTS and XAS. In contrast to the conclusions of Kim and Seff, we could not detect any triazane, either in the pores of the zeolites or in the gas phase by temperature desorption. All alternative attempts to isolate this molecule through adduct formation with BH<sub>3</sub> also failed. No other species could be unambiguously identified by *operando* XAS and DRIFTS. XAS indicates that ammonia is adsorbed onto the 6 ring-centered Ag of the zeolite without the redox reaction. We can conclude that the formation of cyclotriazane by the auto-oxidation of ammonia is unlikely. Consequently, it seems highly unlikely that cyclotriazane synthesis could be carried out by NH<sub>3</sub> treatment of a silver-exchanged LTA zeolite. The synthesis and isolation of the highly reactive cyclotriazane molecule remain a quest for the future.

 Received 8th April 2024,  
 Accepted 22nd January 2025

DOI: 10.1039/d4nj01615g

rsc.li/njc

## Introduction

With the exception of hydrazines and triazanes,<sup>1–4</sup> all sigma-catenated polynitrogen derivatives are scarce despite their potential appeal as ligands, energetic materials and so on.<sup>5–7</sup> Among polyazanes, derivatives of cyclotriazane (general formula N<sub>3</sub>H<sub>3</sub>) are a particularly interesting target, but they present a challenge due to their very high reactivity.<sup>8</sup> Cyclotriazane has been predicted to be stable at room temperature.<sup>9,10</sup> While several methods toward protected variants of cyclotriazane have been introduced,<sup>11–15</sup> N<sub>3</sub>H<sub>3</sub> itself was observed only by Kim and Seff in 1977, through the stoichiometric oxidation of ammonia in a zeolite followed by thermodesorption.<sup>16</sup> More precisely, they reported the synthesis of cyclotriazane and triazane from

ammonia in contact with a single crystal of a silver (Ag<sup>+</sup>)-exchanged LTA zeolite. Based on single-crystal XRD analysis of the crystal, Kim and Seff proposed that cyclotriazane was present and confined in the alpha cavity of the zeolite and in the sodalite cages. They deduced from crystallographic analysis that cyclotriazane is complexed to Ag<sup>+</sup> *via*  $\pi$ -bonding. In addition, the authors confirmed the synthesis of triazane by mass spectroscopy analysis. To the best of our knowledge, however, triazane and, in particular, cyclotriazane has not yet been isolated, perhaps due to their low stability.

In an attempt to synthesize and isolate cyclotriazane for the first time, we reproduced the work of Kim and Seff, starting from a bed of the polycrystalline silver (Ag<sup>+</sup>)-exchanged LTA zeolite. In contrast to the results of Kim and Seff, we were unable to detect any triazane in the gas phase by temperature desorption. All alternative attempts to isolate cyclotriazane by adduct formation with BH<sub>3</sub> also failed. The formation of species other than NH<sub>3</sub> adsorbed onto the silver-exchanged zeolites, as well as the oxidation state of silver species, was investigated by *operando* DRIFTS and XAS.

<sup>a</sup> Université Claude Bernard Lyon1, CNRS, IRCELYON UMR5256, 2 Avenue Albert Einstein, 69626 Villeurbanne Cedex, France.

E-mail: david.farrusseng@ircelyon.univ-lyon1.fr

<sup>b</sup> Université Claude Bernard Lyon 1, CNRS, CNES, Ariane Group, LHCEP, 2 rue Victor Grignard, F-69622 Villeurbanne, France

 † Electronic supplementary information (ESI) available. See DOI: <https://doi.org/10.1039/d4nj01615g>


## Materials and methods

### Silver exchanged zeolite preparation

Molecular sieve 5A and silver nitrate were purchased from Sigma-Aldrich. Na-exchanged 5A zeolite (1.0 g) was dispersed in a 0.5 M aqueous silver nitrate solution (100 mL). The medium was left under stirring (500 rpm) at room temperature for 5 h. Then the medium was filtered and the solid was washed with Milli-Q water. The wash water was tested for silver by adding a few drops of concentrated HCl. The solid was considered to have been properly washed when no precipitate was observed in the wash water. The solid was dried overnight at 80 °C, and then stored in a dark place.

### NH<sub>3</sub> adsorption and product trapping

The experimental setup is shown in Fig. S1 (ESI†). In a U-shaped reactor, silver-exchanged zeolite polycrystalline powder (100 mg) was dehydrated by heating to 400 °C under nitrogen flow at 50 mL min<sup>-1</sup> overnight (for comparison, in the study undertaken by Kim and Seff,<sup>16</sup> crystals were dehydrated at 400 °C under vacuum for three days). After this treatment, the color of the sample changed from white to orange. The sample was then cooled to room temperature under a flow of dry nitrogen. Next, the sample was placed under a stream of ammonia (1800 ppm diluted in N<sub>2</sub>) at 50 mL min<sup>-1</sup> for 48 h. Finally, the sample was placed under nitrogen flow (50 mL min<sup>-1</sup>) and heated in 30-min steps to 40 °C, 70 °C, 100 °C, 120 °C, 150 °C, 200 °C and 250 °C. Outlet flows were bubbled through an entrapment solution containing BH<sub>3</sub>. The flask containing the boron solution was pre-washed and dried overnight (90 °C). The trapping solution was prepared by diluting 15 mL of a 1 M commercial solution of BH<sub>3</sub>-THF (Sigma-Aldrich) in 40 mL of anhydrous THF under an argon atmosphere, and then kept at -85 °C during effluent sequestration. The trapping solution was analyzed using <sup>11</sup>B and <sup>14</sup>N liquid-state NMR on a Bruker AVANCE HD 400 WB spectrometer and using HR ESI mass spectrometry on a Bruker Impact II mass spectrometer.

### Operando FT-IR experiment

The operando DRIFTS experiments were performed using a modified high-temperature DRIFTS cell from Spectra-Tech fitted with KBr windows and placed in a Collector II assembly. The spectrophotometer used was a Nicolet 8700 (Thermo Fisher Scientific) fitted with a liquid-N<sub>2</sub> cooled MCT detector. The DRIFT spectra were recorded at a resolution of 4 cm<sup>-1</sup>, and 16 scans were averaged. The sample was placed on a bed of silicon carbide (SiC) and dehydrated at 300 °C for 3 h under helium flow, followed by cooling to 30 °C. The solid bed was exposed to 1800 ppm ammonia diluted in N<sub>2</sub> for 48 h. FT-IR spectra of the surface were recorded at various times. In the figures below that report the adsorption results, *t*<sub>0</sub> corresponds to the moment when the valve is turned to direct NH<sub>3</sub> flow onto the solid. Ammonia thermodesorption was performed under helium flow. Temperature plateaus of 30 minutes were

achieved. After each plateau, the temperature was lowered to 40 °C to record an FT-IR spectrum of the sample surface.

### Operando XAS experiment

Operando XAS experiments were carried out at the BM30b (CRG-FAME) beamline of the ESRF synchrotron facility. The spectra were acquired at the Ag K edge in the transmission mode, using a Si(220) crystal monochromator. The data were analyzed using FEFF<sup>17</sup> and VIPER<sup>18</sup> programs. The edge background was extracted using Bayesian smoothing. Extended X-ray absorption fine structure (EXAFS) fitting was done alternatively in the *R* and *k* spaces. Coordination numbers (CN), interatomic distances (*R*), distance variance ( $\sigma^2$ ) and energy shifts ( $\Delta E_0$ ) were used as fitting variables.

An Ag-LTA sample pre-activated at 400 °C under N<sub>2</sub> was fed into a tubular reactor and heated under He flow at 300 °C for 30 min, and then cooled to 30 °C under He. The catalytic bed was exposed to a 1% NH<sub>3</sub> flow in He at constant temperature, for 8 h. Next, the zeolite was put back under helium flow and heated to 100 °C for 2 h. XAS spectra were recorded at the various steps of the protocol. The spectra of Ag-LTA samples after different treatments were compared with the results of theoretical simulations. The XANES spectra were simulated using the FDMNES program,<sup>19</sup> in the finite differences mode, using a cluster radius of 6.5 Å. The spectra were convoluted using tabulated core-hole parameters for the Ag K edge. To represent the structures, the Ag<sub>14</sub> cluster inside the sodalite cage from the work of Mayoral *et al.*<sup>20</sup> was modified by attaching small molecules (NH<sub>3</sub>, H<sub>2</sub>O, and OH) to the external Ag atoms (golden atoms in Fig. S19, ESI†). In our model, it was considered that the external silvers are Ag<sup>+</sup> while the internal one are Ag<sup>0</sup>, as reported by Kim and Seff in another study.<sup>21</sup>

The structure proposed by Kim and Seff<sup>16</sup> was followed to generate the simulated spectrum of Ag-N<sub>3</sub>H<sub>3</sub>. The modified structures were optimized by DFT using the Quantum Espresso code and then applied as such for the FDMNES simulations.

## Results

### Synthesis and characterization of silver-exchanged LTA

The silver exchange rate and the Si/Al ratio were determined by X-ray fluorescence spectroscopy (Table S1, ESI†). Almost all Na<sup>+</sup> are exchanged by Ag species (96.8%). The ionic exchange did not modify the Si/Al ratio (1.01).

The diffractograms of the starting zeolite (NaA) and of the material after silver exchange and drying are compared in Fig. S2 (ESI†). Additional peaks were observed in the Ag-LTA diffractogram at 22.8°, 31.8°, 37.1° and 45.2°. Phase identification using EVA crystallographic software and the 2021 powder diffraction file (PDF) database was carried out on the Ag-LTA diffractogram. From this analysis, the Ag-LTA diffractogram was found to match perfectly with a reference solid (A zeolite) fully exchanged with silver (Fig. S3, ESI†). Therefore, the peaks that appear after exchange correspond to the



addition of silver to the zeolite as a cluster in the sodalite cage.<sup>20</sup> Finally, no trace of silver oxide appeared on the diffractograms.

### Attempts to trap triazanes by thermal desorption

In the study by Kim and Seff,<sup>16</sup> a fully exchanged Ag-LTA crystal was dehydrated under vacuum at 400 °C and then treated with ammonia for 40 h. The authors claimed to have detected the molecular peaks of  $\text{N}_3\text{H}_3^+$  and  $\text{N}_3\text{H}_2^+$  using mass spectroscopy after heating the zeolite to 70 °C. We reproduced this ammonia adsorption/desorption experiment based on this protocol but using polycrystalline powder. In a tubular reactor, Ag-LTA that had previously been dehydrated at 400 °C under dry  $\text{N}_2$  was treated with 1800 ppm ammonia for 48 hours. *Via* this treatment, the saturation of the sample surface with ammonia is ensured. To confirm this, a breakthrough curve was recorded under the same adsorption conditions (Fig. S4, ESI<sup>†</sup>). The concentration at the column outlet returned to the inlet flow value after 2.5 h under flow conditions.

Surface species were desorbed under nitrogen flow and in temperature steps between 25 °C and 250 °C. We were unable to detect cyclotriazane ( $m/z$   $\text{N}_3\text{H}_2^+ = 44$ ) in the outlet stream by gas-phase mass spectrometry. As we hypothesized that cyclotriazane could be decomposed before the MS detector, we tried to stabilize it at the outlet of the bed. This method was based on the use of boron in the borane form ( $\text{BH}_3$ ), as a Lewis acid, to form borane–amine adducts to entrap and stabilize potentially sensitive nitrogen products. The borane solution was kept at –85 °C to prevent the degradation of the adducts formed. Borane–amine adduct formation is well identified by <sup>11</sup>B NMR analysis, with the emergence of a signal at a chemical shift that depends on the nature of the amine. While the majority of boron is present as a  $\text{BH}_3$ –THF adduct (signal at  $\approx 0$  ppm), other species coexist in the solution (Fig. S5–S7, ESI<sup>†</sup>). No signals other than those induced by ammonia

trapping appeared after the adsorption–desorption experiment on Ag-LTA zeolite (Fig. S8 and S9, ESI<sup>†</sup>).

In the case where different boron adducts would result in an overly small shift on the <sup>11</sup>B spectra, <sup>14</sup>N NMR spectra of the trapping solution after adsorption–desorption and blank tests were recorded (Fig. S10, ESI<sup>†</sup>). The same signals can be observed for the two samples (–26, –38 and –60 ppm). These signals correspond to nitrogen in  $\text{BH}_3$ – $\text{NH}_3$  and borazine, in agreement with the <sup>11</sup>B NMR results.<sup>22,23</sup>

The trapping solution was also analyzed by high-resolution electrospray ionization mass spectrometry (ESI-MS). Prior to analysis, the sample was diluted in a solvent mixture to facilitate species ionization. This dilution solvent contained methanol, water, dichloromethane and formic acid. An analysis of the commercial  $\text{BH}_3$  solution was carried out to deduce the contribution of the environment (Fig. S11, ESI<sup>†</sup>). Analyses of the trapping solution after adsorption and desorption of ammonia on the Ag-LTA sample (and of a blank test obtained from ammonia bubbling) were also carried out (Fig. 1). A characteristic signal is observed at  $m/z$  47.08 u, corresponding to  $[\text{BH}_3\text{–N}_2\text{H}_4]\text{–H}^+$ . However, this signal does not suggest that ammonia was oxidized upon contact with the zeolite, since this signal was also found in the analysis of  $\text{NH}_3$ – $\text{BH}_3$ . This suggests that hydrazine is formed during the analysis, most likely during the ionization step, when  $\text{NH}_3$  is contained in the sample. By comparing the mass spectra, we note that no characteristic signal appears during the experiment with Ag-LTA zeolite. Thus, no molecules other than ammonia were desorbed from the material after the experiment.

In summary, despite using different analytical approaches (online MS, trapping and analysis by NMR and MS), no species other than ammonia were detected after temperature-programmed desorption of  $\text{NH}_3$ -loaded silver-exchanged zeolites. We thus conclude that if triazane or cyclotriazane was to exist in the zeolite, it would decompose in the gas, but could

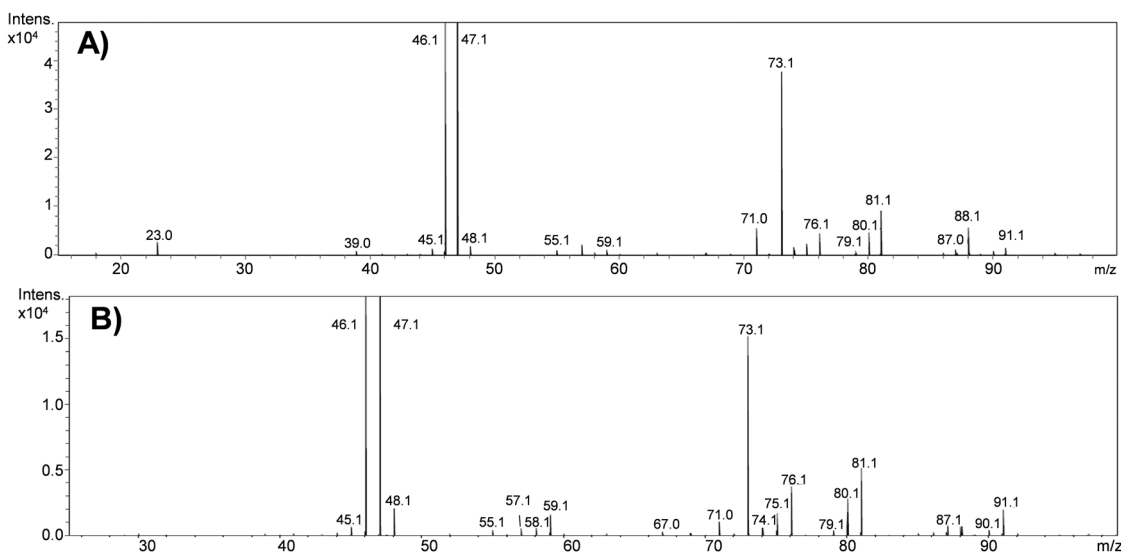


Fig. 1 HR ESI mass spectra of (A) the trapping solution after adsorption/desorption of ammonia on Ag-LTA, and (B) the trapping solution after a bubbling of ammonia for 6 h.



perhaps be stabilized by Ag clusters in the zeolite framework. Hence, our further efforts were aimed at the identification of any nitrogen species possibly formed in the zeolite.

### Operando DRIFTS ammonia adsorption results

The DRIFT spectra of surface species on Ag-LTA upon  $\text{NH}_3$  uptake as a function of time are compiled in Fig. S16 (ESI<sup>†</sup>). Adsorption signals between  $3600\text{ cm}^{-1}$  and  $3250\text{ cm}^{-1}$ , and a peak around  $1600\text{ cm}^{-1}$ , are also found for Na-LTA and thus correspond to the adsorption of  $\text{NH}_3$  (Fig. S12, ESI<sup>†</sup>). The appearance of these peaks is immediate upon  $\text{NH}_3$  exposure, indicating very fast adsorption of  $\text{NH}_3$  in the zeolite pores.

In contrast, a band at  $1337\text{ cm}^{-1}$  appears only after 30 min under  $\text{NH}_3$  flow. Moreover, it exhibits an initial appearance rate around 15 times slower than the signals corresponding to  $\text{NH}_3$  adsorption (Fig. 2). DRIFT spectra of Ag-LTA during thermo-controlled desorption are shown in Fig. S17 (ESI<sup>†</sup>). The relative areas of the bands at  $3300$  and  $1337\text{ cm}^{-1}$  are plotted as a function of desorption temperature in Fig. S18 (ESI<sup>†</sup>). The intensity of the band at  $1337\text{ cm}^{-1}$  is very sensitive to temperature, whereas the signal at  $3300\text{ cm}^{-1}$  associated with  $\text{NH}_3$  is much less sensitive. The band of the unidentified species at  $1337\text{ cm}^{-1}$  decreases by 60% at  $40\text{ }^\circ\text{C}$  and completely vanishes at  $100\text{ }^\circ\text{C}$ . Generally speaking, the vanishing of a signal when the temperature increases may arise from either the desorption of the species or a modification of the structure of the adsorbed species. However, there is insufficient evidence to conclude that N–N bonds may have been formed.

### XAS spectroscopy

In 2016, Seff *et al.* reviewed silver chemistry in zeolites, discussing the 1977 experiment anew.<sup>24</sup> In this article, they proposed two reaction equations to describe the formation of triazines and cyclotriazines, according to two reaction paths in which silver is either a catalyst or a reactant. In the silver ion catalyst hypothesis, they propose that the incomplete coordination of the  $\text{Ag}^+$  ion by the zeolite would promote the formation of an active intermediate for the catalysis of the oxidative coupling of ammonia. According to the authors, the formation of triazines and cyclotriazines is achieved by the confined  $\text{Ag}^+$

and  $\text{Ag}^0$  sites in sodalite cages. They claimed to have observed  $\text{N}_3\text{H}_3$  in the alpha cage complexed onto the 6 ring-centered Ag (Fig. S20, ESI<sup>†</sup>). We assume that the formation of this complex can be detected by *operando* XAS analyses, as a particular modification of the Ag coordination state. Furthermore, if silver acts as an oxidant, the detection of a change in the oxidation state of the metal would indicate that the reaction has occurred.

The experimental XAS curves and the calculated spectra are presented in Fig. 3. *In situ* dehydration ( $100\text{ }^\circ\text{C}$  under He) was also monitored by XAS (Fig. S21, ESI<sup>†</sup>). A white line intensity is observed on the hydrated solid which does not appear for the dried sample. This causes the partial reduction of silver during the dehydration. The position of the Ag K edge main jump does not depend significantly on the Ag oxidation state, as observed previously in several studies.<sup>25–27</sup> However, the position and intensity of the white line, as well as the overall shape of the XANES profiles, vary noticeably. Significant differences are observed between the XANES profiles of the initial, ammonia-treated and helium-treated solids. In the XAS spectra recorded on Ag-LTA before and after  $\text{NH}_3$  adsorption, a shift in the white line from  $25\,529.7$  to  $25\,532.7\text{ eV}$  can be observed. However, the white line is at  $25\,529.7\text{ eV}$  in Ag-LTA after desorption treatment under He. So, from the point of view of the silver atoms in the zeolite, ammonia adsorption and desorption are globally reversible. No permanent reduction in the silver content was observed after treatment with ammonia. The variations of the observed XANES profiles agree with the FDMNES calculations. The high-energy shift of the white line maximum is observed between the simulated spectra of Ag and  $\text{Ag-NH}_3$ . Note that the variations in the spectra are attenuated by the core Ag cluster inside the sodalite cage, which remains unchanged during the ammonia treatment. The simulated spectrum of silver complexed with cyclotriazine as proposed by Kim and Seff gives a very distinctive profile compared to  $\text{Ag-NH}_3$ . Unfortunately, no contribution of  $\text{N}_3\text{H}_3$  was found in the experimental XAS spectrum. Thus, the structure of cyclotriazine complexed with 6 ring-centered Ag was not observed after ammonia treatment of Ag-LTA.

## Discussion

In light of the results obtained, we doubt whether it is possible to isolate triazine or cyclotriazine based on the observation and method proposed by Kim and Seff. We did indeed observe MS signals at 46 and 48 u that correspond to  $[\text{N}_3\text{H}_3]\text{-H}^+$  and  $[\text{N}_3\text{H}_5]\text{-H}^+$ , but they are also present for a pure  $\text{NH}_3$  stream (*i.e.*, in the absence of Ag-LTA). Hence, we cannot provide evidence of the synthesis of triazine in Ag-LTA. Unfortunately, the MS technology used in 1977 was different, and it is difficult to determine whether an analytical bias may have been behind Kim and Seff's observation.

On the other hand, *operando* DRIFTS experiments may reveal the formation of a novel species, as its appearance is delayed with respect to the adsorption of  $\text{NH}_3$ , and thus is likely a consecutive step. The vanishing of this signal under heat

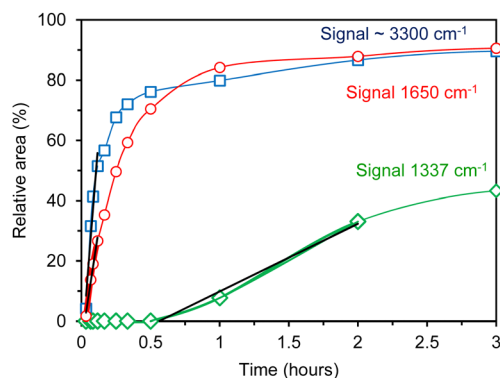


Fig. 2 Kinetics of signal appearance during the adsorption of  $\text{NH}_3$  on Ag-LTA (from the IR spectra in Fig. S16, ESI<sup>†</sup>).



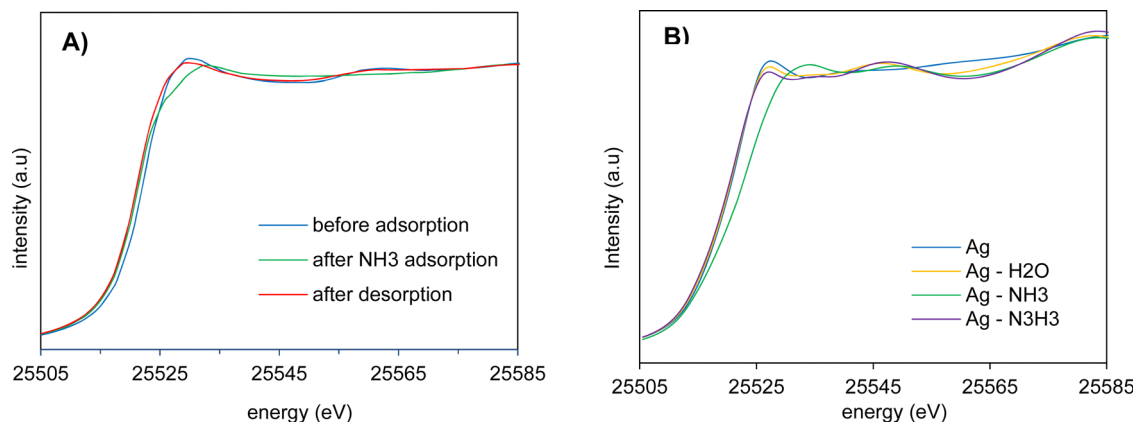


Fig. 3 (A) *Operando* XAS spectra of Ag-LTA under He before  $\text{NH}_3$  adsorption (dried), after  $\text{NH}_3$  adsorption and after desorption by heating at  $100\text{ }^\circ\text{C}$  under He. (B) Simulated XAS spectra of silver cluster in sodalite with addition of  $\text{H}_2\text{O}$  (yellow),  $\text{NH}_3$  (green) and  $\text{N}_3\text{H}_3$  (purple) on the 6 ring-centered silver atoms (Fig. S19, ESI $^\dagger$ ).

treatment at low temperature may indicate a facile desorption or degradation of the species. Unfortunately, we could not identify the vibration that is associated with the band at  $1337\text{ cm}^{-1}$ .

On the other hand, *operando* XAS analysis of Ag-LTA under  $\text{NH}_3$  flow revealed that no species other than ammonia were present in the vicinity of the silver atoms.

In our XAS experiment, ammonia was adsorbed onto the zeolite, particularly onto the 6 ring-centered Ag, and was then desorbed by heating to  $100\text{ }^\circ\text{C}$  under He with no irreversible redox reaction with silver being observed.<sup>28–36</sup>

In the review by Seff *et al.*, the team proposed the synthesis of cyclotriazane by auto-oxidation of ammonia in which the silver ions are only a catalyst. The Gibbs free enthalpy of the equation proposed by the team was then calculated. In these calculations, all species are considered in the gas phase. This hypothesis is consistent with Seff's 1977 study, in which triazane and cyclotriazane were detected after desorption of the zeolite. The Gibbs standard free enthalpy and the thermodynamic data used are compiled in Table S2 (ESI $^\dagger$ ). At  $100\text{ }^\circ\text{C}$ , the Gibbs standard free enthalpy is positive. Therefore, the formation of cyclotriazane by the auto-oxidation of ammonia seems very unlikely. The lack of a redox reaction of silver supports the absence of cyclotriazane in the zeolite.

As a result, it would appear that the unidentified signal observed in the *operando* DRIFTS experiments is not related to an unknown species adsorbed on silver but more likely to the adsorption of ammonia at high loading ( $\text{NH}_3$ – $\text{NH}_3$  interaction).

## Conclusions

The synthesis protocol proposed by Kim and Seff in 1977 was reproduced in order to isolate cyclotriazane. The trapping experiments revealed that only ammonia was present downstream of the silver-exchanged zeolite after ammonia treatment. The detection of cyclotriazane adsorbed on the Ag surface of the material was attempted by *operando* DRIFTS and XAS experiments. These analyses suggest that only

ammonia was present on the zeolite surface and in the vicinity of the silver atoms. No other species could be unambiguously identified. Consequently, it seems highly unlikely that cyclotriazane synthesis could be carried out by  $\text{NH}_3$  treatment of a silver-exchanged LTA zeolite. The synthesis and isolation of the highly reactive cyclotriazane molecule remain a quest.

## Author contributions

R. B.: investigation, methodology, writing – original draft, writing – review & editing. P. A.: investigation, formal analysis, writing – review & editing. E. L.: conceptualization, supervision, funding acquisition, writing – review & editing. D. F.: conceptualization, supervision, funding acquisition, writing – review & editing.

## Data availability

Raw data were generated at IRCELYON. Derived data supporting the findings of this study are available from the corresponding author D. F. on request.

## Conflicts of interest

There are no conflicts to declare.

## Acknowledgements

The authors thank the Centre National d'Etudes Spatiales (CNES) for funding.

## Notes and references

- 1 K. Linke and H. J. Göhausen, *Chem. Ber.*, 1971, **104**, 301–306.
- 2 N. Egger, L. Hoesch and A. S. Dreiding, *Helv. Chim. Acta*, 1983, **66**, 1416–1426.



- 3 T. Kanzian and H. Mayr, *Chem. – Eur. J.*, 2010, **16**, 11670–11677.
- 4 A. Glowacki, V. Jeux, G. Gasnier, L. Joucla, G. Jacob and E. Lacôte, *Synlett*, 2018, 566–570.
- 5 W. H. Pirkle and P. L. Gravel, *J. Org. Chem.*, 1978, **43**, 808–815.
- 6 B. Krumm, A. Vij, R. J. Kirchmeier, J. M. Shreeve and H. Oberhammer, *Angew. Chem., Int. Ed. Engl.*, 1995, **34**, 586–588.
- 7 K. L. Martin and G. W. Breton, *Acta Crystallogr., Sect. C: Struct. Chem.*, 2017, **73**, 660–666.
- 8 A. Karahodza, K. J. Knaus and D. W. Ball, *J. Mol. Struct. THEOCHEM*, 2005, **732**, 47–53.
- 9 M.-T. Nguyen, J. Kaneti, L. Hoesch and A. S. Dreiding, *Helv. Chim. Acta*, 1984, **67**, 1918–1929.
- 10 D. H. Magers, E. A. Salter, R. J. Bartlett, C. Salter, B. A. Hess and L. J. Schaad, *J. Am. Chem. Soc.*, 1988, **110**, 3435–3446.
- 11 C. Leuenberger, L. Hoesch and A. S. Dreiding, *J. Chem. Soc., Chem. Commun.*, 1980, 1197–1198.
- 12 L. Hoesch, C. Leuenberger, H. Hilpert and A. S. Dreiding, *Helv. Chim. Acta*, 1982, **65**, 2682–2696.
- 13 A. R. Katritzky, K. Burger, U. Wucherpfennig and E. Brunner, *Fluoro Heterocycles with Five-Membered Rings, Advances in Heterocyclic Chemistry*, 1994, vol. 60, pp. 1–64, DOI: [10.1016/S0065-2725\(08\)60181-6](https://doi.org/10.1016/S0065-2725(08)60181-6).
- 14 R. Gleiter, C. Sigwart, H. Irngartinger and S. Gries, *Tetrahedron Lett.*, 1988, **29**, 185–188.
- 15 W. Marterer, O. Klingler, R. Thiergardt, E. Beckmann, H. Fritz and H. Prinzbach, *Chem. Ber.*, 1991, **124**, 621–633.
- 16 Y. Kim and K. Seff, *J. Am. Chem. Soc.*, 1977, **99**, 7057–7059.
- 17 A. L. Ankudinov, C. E. Bouldin, J. J. Rehr, J. Sims and H. Hung, *Phys. Rev. B: Condens. Matter Mater. Phys.*, 2002, **65**, 104107.
- 18 K. V. Klementev, *J. Synchrotron Radiat.*, 2001, **8**, 270–272.
- 19 O. Bunău and Y. Joly, *J. Phys.: Condens. Matter*, 2009, **21**, 345501.
- 20 A. Mayoral, T. Carey, P. A. Anderson and I. Diaz, *Microporous Mesoporous Mater.*, 2013, **166**, 117–122.
- 21 Y. Kim and K. Seff, *J. Am. Chem. Soc.*, 1978, **100**, 6989–6997.
- 22 *Nuclear Magnetic Resonance Spectroscopy of Boron Compounds*, ed. H. Nöth and B. Wrackmeyer, Springer Berlin Heidelberg, Berlin, Heidelberg, 1978.
- 23 S. De Angelis, P. Celestini, G. Rebuzzini, L. Degennaro and R. Luisi, *Synthesis*, 2017, 1969–1971.
- 24 N. H. Heo, Y. Kim, J. J. Kim and K. Seff, *J. Phys. Chem. C*, 2016, **120**, 5277–5287.
- 25 N. D. Leifer, A. Colon, K. Martocci, S. G. Greenbaum, F. M. Alamgir, T. B. Reddy, N. R. Gleason, R. A. Leising and E. S. Takeuchi, *J. Electrochem. Soc.*, 2007, **154**, A500.
- 26 C. Fan, Q. Li, B. Chu, G. Lu, Y. Gao and L. Xu, *Phys. Chem. Miner.*, 2018, **45**, 679–693.
- 27 B. A. Manning, S. R. Kanel, E. Guzman, S. W. Brittle and I. E. Pavel, *J. Nanopart. Res.*, 2019, **21**, 213.
- 28 S. Aguado, G. Bergeret, C. Daniel and D. Farrusseng, *J. Am. Chem. Soc.*, 2012, **134**, 14635–14637.
- 29 C. Daniel, A. Elbaraoui, S. Aguado, M.-A. Springuel-Huet, A. Nossov, J.-P. Fontaine, S. Topin, T. Taffary, L. Deliere, Y. Schuurman and D. Farrusseng, *J. Phys. Chem. C*, 2013, **117**, 15122–15129.
- 30 M. Zaarour, M. El Roz, B. Dong, R. Retoux, R. Aad, J. Cardin, C. Dufour, F. Gourbilleau, J.-P. Gilson and S. Mintova, *Langmuir*, 2014, **30**, 6250–6256.
- 31 L. Deliere, S. Topin, B. Coasne, J.-P. Fontaine, S. De Vito, C. Den Auwer, P. L. Solari, C. Daniel, Y. Schuurman and D. Farrusseng, *J. Phys. Chem. C*, 2014, **118**, 25032–25040.
- 32 E. Fron, S. Aghakhani, W. Baekelant, D. Grandjean, E. Coutino-Gonzalez, M. Van der Auweraer, M. B. J. Roeflaers, P. Lievens and J. Hofkens, *J. Phys. Chem. C*, 2019, **123**, 10630–10638.
- 33 J. M. Rimsza, K. W. Chapman and T. M. Nenoff, *J. Phys. Chem. C*, 2020, **124**, 4517–4524.
- 34 X. Hu, J. Bai, C. Li, H. Liang and W. Sun, *Eur. J. Inorg. Chem.*, 2015, 3758–3763.
- 35 M. El-Roz, I. Telegeiev, N. E. Mordvinova, O. I. Lebedev, N. Barrier, A. Behilil, M. Zaarour, L. Lakiss and V. Valtchev, *ACS Appl. Mater. Interfaces*, 2018, **10**, 28702–28708.
- 36 H. I. Hamoud, F. Douma, M. Lafjah, F. Djafri, O. Lebedev, V. Valtchev and M. El-Roz, *ACS Appl. Nano Mater.*, 2022, **5**, 3866–3877.

